Value of zeolites in asymmetric induction during photocyclization of pyridones, cyclohexadienones and naphthalenones†

Karthikeyan Sivasubramanian, Lakshmi S. Kaanumalle, Sundararajan Uppili and V. Ramamurthy*

Received 19th February 2007, Accepted 26th March 2007
First published as an Advance Article on the web 23rd April 2007
DOI: 10.1039/b702572f

Two strategies, namely chiral inductor and chiral auxiliary approaches, have been examined within zeolites with the aim of achieving asymmetric induction during the photocyclization of cyclohexadienone, naphthalenone and pyridone derivatives. Within zeolites, enantioselectivity as high as 55% and diastereoselectivity as high as 88% have been obtained. The observed stereoselectivities are significant given the fact that these reactions gave very little stereoselectivities in isotropic solution media. The results obtained on the photocyclization of dienones, naphthalenones and *N*-alkyl pyridones within zeolites compliment our earlier investigations on the photocyclization of tropolone derivatives, the geometric isomerization of 1,2-diphenylcyclopropanes and 2,3-diphenyl-1-benzoyl cyclopropanes, and the Norrish type II reaction of α-oxoamides, phenyl adamantyl ketones, phenyl norbornyl ketones and phenyl cyclohexyl ketones. With the help of these examples, we have established the importance of zeolite and its charge compensating cations in effecting asymmetric induction in photochemical reactions.

Introduction

The chiral sources that have been employed to achieve stereoselectivity in photochemical reactions include circularly polarized light, chiral sensitizers, chiral solvents, chiral substituents, chiral host–guest assemblies and chiral crystalline environments.[1–8] In our laboratory, an approach based on solid host–guest assemblies using zeolite as the solid host to induce asymmetric induction during photochemical transformations has been developed.[9] We have previously demonstrated that the confined cavities of a zeolite and charge compensating cations present within them could be used to induce enantio- and diastereoselectivity in products of photoreactions such as geometric isomerization, hydrogen abstraction and cyclization.[10] To establish generality of the zeolite-based approach, we have investigated excited state reactions of 3,3-dimethyl-4-oxo-3,4-dihydronaphthalene derivatives (**1a**, **1b**, **2a–2e**, **2g**, **2i**, **2j**, **2m–2q**, **2s**, **2t**), 2,4 cyclohexadienone derivatives (**1c**, **1d**, **4a**, **4e–4h**, **4j**, **4n**, **4o**, **4q**, **4r**, **4s**) and *N*-alkyl pyridone derivatives (**1e–1j**, **6e**, **6g**, **6i–6q**) (Schemes 1–4) within MY zeolites where M is an alkali ion. Results obtained with these examples are presented in this report.

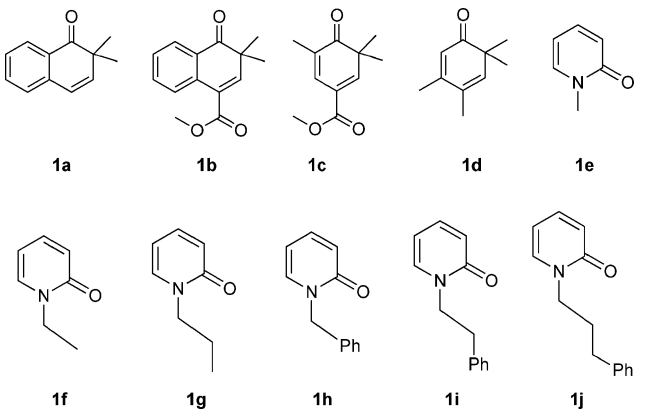

Scheme 1 Naphthalenone, dienone and pyridone derivatives investigated by the chiral inductor approach.

Results

In order to establish the value of zeolites during asymmetric induction in photoreactions, we have pursued two approaches, namely chiral inductor approach—*i.e.* inclusion of an achiral reactant within a chirally-modified zeolite and chiral auxiliary approach—*i.e.* inclusion of a reactant molecule covalently appended with a chiral inductor within an achiral zeolite. Photoproducts were analyzed by either GC or HPLC using chiral columns. The first of the two enantiomeric/diasteromeric peaks on GC/HPLC traces was assigned as A and the second peak as B. In the present manuscript, we disclose the results that we believe would convince the readers that the zeolite-based strategy is a viable (although not general) approach to achieve asymmetric induction in photoreactions.

Chiral inductor approach

Structures of four achiral dienones and six pyridones examined in the context of chiral inductor approach are provided in Scheme 1. It has been established earlier that naphthalenone[11] and 2,4-cyclohexadienone[12] derivatives upon irradiation in highly polar solvents such as trifluoroethanol undergo oxa di-π-methane rearrangement from a ππ* excited triplet state (Scheme 2). We have previously shown that the lowest excited state of α,β-enones

Department of Chemistry, University of Miami, Coral Gables, Fl 33124, USA

† Electronic supplementary information (ESI) available: Experimental details including synthesis, characterization of reactants and photoproducts and analysis conditions for photoproducts. See DOI: 10.1039/b702572f

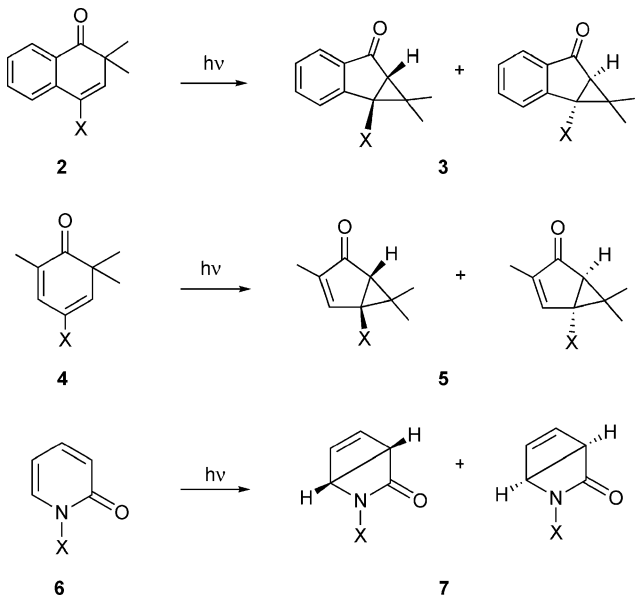

Scheme 2 Photochemistry of chiral auxiliary appended naphthalenone, dienone and pyridone derivatives. X in structures **2** and **4** corresponds to COR* and in structure **6** corresponds to CH_2COR*. The structures of chiral auxiliaries (R* in X) used during chiral auxiliary approach are provided in Scheme 4.

is ππ* within alkali ion exchanged MY zeolites.[13] Consistent with this, oxa di-π-methane rearrangement products alone were obtained upon irradiation of **1a–d** included within a chirally-modified zeolite. In agreement with the known photobehavior of pyridones (Scheme 2),[14–19] excitation of *N*-alkyl pyridone derivatives (**1e–1j**) adsorbed within chirally-modified zeolites gave

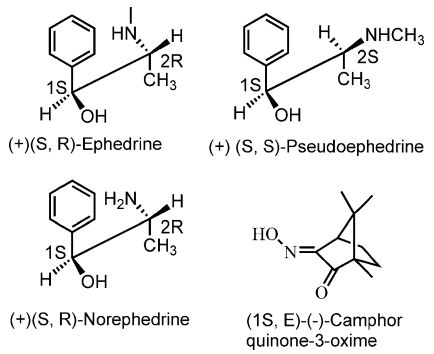

Scheme 3 Optically pure chiral inductors used.

chiral β-lactams. The zeolite used for the current study is the commercially available achiral Y zeolite. The chiral environment was created by inclusion of chiral inductor molecules into the supercages of MY zeolite. Experimental procedures including adsorption, irradiation, extraction and analysis are described in the experimental section.

In the chiral inductor approach, in order to maximize the chances of the reactant molecule being closer to the chiral inductor molecule, we used a higher ratio of chiral inductor to the reactant (10 : 1). Structures of the chiral inductors used in this study are shown in Scheme 3. Results obtained in the presence of these chiral inductors are presented in Table 1. Irradiation of various dienone and pyridone derivatives within chirally-modified NaY zeolites, resulted in moderate enantiomeric excess (ee) in the photoproducts. The importance of chiral inductors and cations present in a zeolite during asymmetric induction was realized from the following observations: (a) irradiation of dienones (**1a–1d**) and pyridones (**1e–1j**) in MY zeolite without a chiral inductor gave

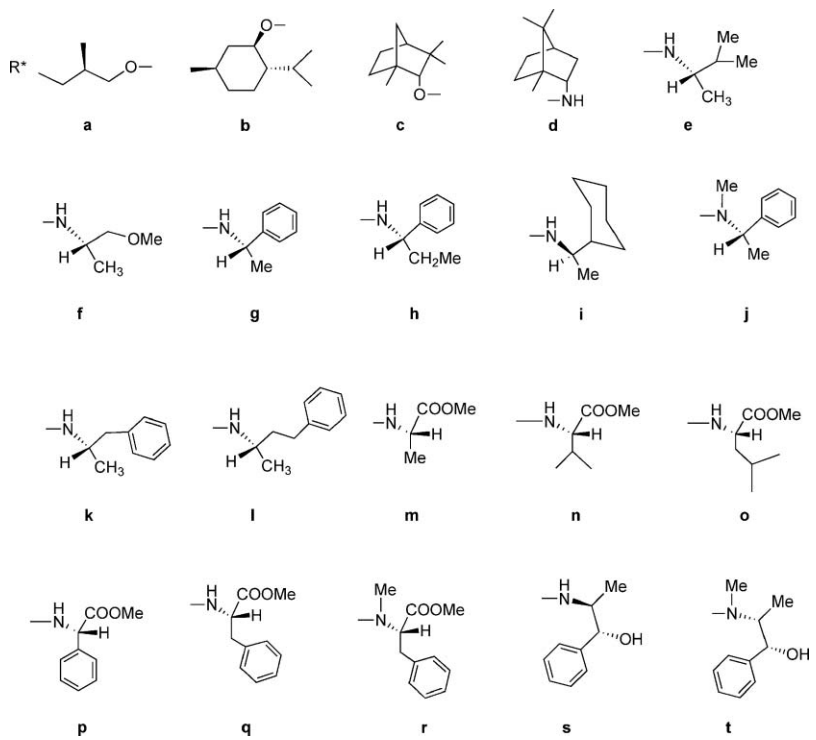

Scheme 4 The structures of chiral auxiliaries used. See Scheme 2 to track the structures to which these groups would be attached.

Table 1 Enantioselectivity in the photoproducts obtained within MY zeolites[a,b,c]

Substrate	Zeolite	Chiral inductor	% Enantiomeric excess
1a	NaY	(−)-Ephedrine	13A
1a	NaY	(+)-Ephedrine	10B
1a	NaY	(+)-Pseudoephedrine	17A
1a	NaY	(−)-Pseudoephedrine	15B
1b	NaY	(−)-Ephedrine	18B
1b	NaY	(+)-Ephedrine	15A
1b	NaY	(+)-Pseudoephedrine	17B
1b	NaY	(−)-Pseudoephedrine	14A
1c	NaY	(1*S*, *E*)-(−)-Camphor quinine-3-oxime	25A
1d	NaY	(−)-Ephedrine	30B
1d	NaY	(+)-Ephedrine	28A
1d	NaY	(−)-Pseudoephedrine	20B
1d	NaY	(+)-Pseudoephedrine	26A
1e	NaY	(−)-Norephedrine	3B
1f	NaY	(−)-Norephedrine	6B
1g	NaY	(−)-Norephedrine	6B
1h	NaY	(−)-Norephedrine	22B
1i	KY	(−)-Ephedrine	53B
1i	RbY	(−)-Ephedrine	40B
1j	NaY	(−)-Norephedrine	50B

[a] A refers to first peak eluting from GC/HPLC column. [b] The optical antipode of the chiral inductor gave the other enantiomer in excess. [c] The loading, irradiation and extraction procedures are provided in the experimental section.

racemic products; (b) irradiation of pyridone **1j** in NaY zeolite with (Si : Al = 40), a zeolite with lesser number of cations gave only 2% enantioselectivity, while the same substrate in NaY (Si : Al = 2.4) with a higher number of cations gave 50% enantioselectivity. Also dienone **1c** while in NaY gave 30% ee, within ephedrine-modified Y-sil (Si : Al > 285), a zeolite with no cation, gave racemic products; (c) the enantioselectivity was also dependent on the nature of the alkali ion present in a zeolite. For example, in the case of **1c**, irradiation in (−)-ephedrine-modified alkali ion exchanged Y zeolites led to an ee of 0% in LiY, 32% in NaY, 26% in KY, 5% in RbY, 0% in CsY and for **1i**, 23% in LiY, 5% in NaY, 53% in KY, 40% in RbY, and 12% in CsY; (d) consistent with the suggestion that interaction between the cation, chiral inductor and reactant molecules plays a crucial role, inclusion of water molecules that would coordinate to the cation, into (−)-ephedrine-modified NaY zeolite reduced the enantioselectivity to 0% from 25% in the case of **1d**; (e) variation of the irradiation temperature had a distinct effect on the enantioselectivity obtained from the product formed from cyclohexadienone derivative (**1d**) (chiral inductor = (−)-ephedrine). Decreasing the temperature from 25 °C to −55 °C increased the enantioselectivity from 30 (B) to 49 (B).

Chiral auxiliary approach

We admit that the enantioselectivity obtained by the chiral inductor approach with the substrates (**1a–1j**) was moderate at best. One way to enhance the chiral environment is to covalently link the chiral inductor to the substrate of interest so that the achiral reactant and chiral inductor components of the same molecule would stay close to each other. We call this chiral auxiliary approach. The chiral auxiliaries used were optically pure chiral alcohols, amines, amino alcohols and amino acid methyl ester derivatives (Scheme 4). Such chiral auxiliary linked naphthalenone (**2**) and cyclohexadienone derivatives (**4**), upon irradiation in solution gave products of oxa di-π-methane rearrangement in less than 13% diastereomeric excess (de). The same substrates when irradiated within NaY zeolite gave products in moderate to high diastereoselectivity (30–81%) (Tables 2 and 3). Similar enhancement in de (∼88%) was observed during the photocyclization of pyridone derivatives (**6**) within MY zeolites (Table 4).

Like in the chiral inductor approach, the diastereoselectivity obtained within MY zeolites varied with the nature of the charge-compensating cations. For example, the naphthalenone derivative **2g** gave the photoproduct (**3g**) with de of 42% (B) in LiY; 48% (B) in NaY; 81% (B) in KY and 46% (B) in RbY. Yet another notable feature was that the nature of the cation not only controlled the extent of diastereoeselectivity but in some cases it also controlled the diastereomer being enhanced. For pyridone derivatives **6l** and **6m**, LiY and NaY gave one diastereomer in excess whereas in KY, RbY and CsY gave the other diastereomer in excess (**6l**: LiY 48% (B), NaY 25% (B), KY 76% (A), RbY 88% (A) and CsY 82% (A); **6m**: LiY 32% (B), NaY 50% (B), KY 36% (A), RbY 25% (A) and CsY 29% (A)). The dienone derivatives (**4f**, **4h**, **4o** and **4q**) also behaved in a similar fashion (Tables 3 and 4). These derivatives

Table 2 Diastereoselectivity in the photoproducts obtained within MY zeolites for naphthalenone derivatives (**2**)[a,b]

Substrate	CH_3CN	NaY	KY	MY
2a	0	10A	8B	31A (LiY)
2b	9B	46A	60A	48A (RbY)
2c	3B	57B	34B	24B (CsY)
2d	13B	48B	35B	34B (RbY)
2e	6	45B	23B	35B (CsY)
2g	0	48B	81B	46B (RbY)
2i	3B	35B	58B	45B (CsY)
2j	8B	13B	13B	25B (LiY)
2m	9A	21A	43A	10A (RbY)
2n	0	12A	58A	20A (RbY)
2o	2A	0	45A	10A (RbY)
2p	8A	5B	41B	5B (RbY)
2q	8A	11B	30B	7B (RbY)
2s	9A	48A	12A	15A (RbY)
2t	6B	19B	57B	30B (LiY)

[a] A refers to first peak eluting from GC/HPLC column. [b] The loading, irradiation and extraction procedures are provided in the experimental section.

Table 3 Diastereoselectivity in the photoproducts obtained within MY zeolites for cyclohexadienone derivatives (**4**)[a,b]

Substrate	CH_3CN	NaY	RbY	MY
4a	2B	5B	12B	22B (CsY)
4e	0	2	38B	31B (CsY)
4f	0	73A	25B	40A (LiY)
4g	5	59A	39B	17A (LiY)
4h	0	41A	13B	34A (LiY)
4j	0	20A	8A	39A (LiY)
4n	4A	53A	7B	32A (LiY)
4o	2A	22A	40B	25A (LiY)
4q	4B	25A	17B	35B (KY)
4r	29A	27A	43A	60A (KY)
4s	11A	59B	18B	25B (KY)

[a] A refers to first peak eluting from GC/HPLC column. [b] The loading, irradiation and extraction procedures are provided in the experimental section.

Table 4 Diastereoselectivity in the photoproducts obtained for pyridone derivatives (**6**) within MY zeolites[a,b]

Substrate	CH_3CN	NaY	KY	MY
6e	1B	44B	75B	38B (RbY)
6g	2B	8A	42A	32A (RbY)
6i	2B	5A	1A	24A (LiY)
6j	3B	84B	74B	64B (CsY)
6k	3B	11B	67B	60B (RbY)
6l	3B	25B	76A	88A (RbY) 82A (CsY)
6m	1A	50B	36A	32B (LiY)
6n	2A	14B	16B	53A (RbY)
6o	1A	33B	10B	28B (LiY)
6p	2B	4A	8A	33B (LiY)
6q	3A	21A	78A	34A (RbY)

[a] A refers to first peak eluting from GC/HPLC column. [b] The loading, irradiation and extraction procedures are provided in the experimental section.

in LiY and NaY gave one diastereomer in excess, whereas in KY, RbY and CsY gave the other diastereomer in excess (Table 3).

Water, as observed in the case of the chiral inductor approach, reduced the de. The diastereoselectivities obtained by irradiation of naphthalenone derivatives (**2b–2e**, **2i** and **2g**) and pyridone derivative (**6l**) under dry and wet conditions are provided in Table 5. These results clearly illustrate the role of free cations in controlling the extent of diastereoselectivity.

Once again, the importance of the cation became evident when diastereoselectivity was monitored for substrate (**6l**) in zeolites having Si : Al ratio of 6 (cations per unit cell = 22), 15 (cations per unit cell = 9) and 40 (cations per unit cell = 3.4). The diastereoselectivity observed for substrate **6l** within KY (Si : Al = 2.4) was 76%. This value decreased to 6% when KY (Si : Al = 40) was used. Zeolite KY with Si : Al ratio of 6 and 15 gave diastereoselectivity of 20% and 10%, respectively. When pyridone derivative **6l** adsorbed onto silica that does not have any cations was irradiated the de was 3%.

Not all chiral auxiliaries were equally effective. Perusal of Tables 2 to 4 suggests that chiral auxiliaries having an aromatic group give better diastereoselectivity than the ones with an alkyl group. For example, irradiation of substrate **2g** gave the photoproduct in 81% de in KY zeolite, whereas irradiation of **2i** gave the photoproduct in only 58% de in KY zeolite. Dienone and pyridone derivatives also exhibited similar behavior. For example, photoirradiation of pyridone derivatives **6g**, **6k** and **6l** gave the β-lactam photoproduct in 42% de in KY zeolite, 67% in KY zeolite and 88% in RbY zeolite, whereas substrate **6i** which has an alkyl chiral auxiliary (cyclohexylethylamine) gave the β-lactam product in 24% de in LiY zeolite. The above comparison revealed that the functional group present in a chiral auxiliary has a role to play in the chiral induction process.

Also to ensure that the observed enhancement in diastereoselectivity within zeolite is not due to any experimental artifacts, the 1 : 1 diastereomeric mixture of photoproducts isolated from solution irradiation of the naphthalenone derivative **2g** was included within NaY by stirring in hexane for 12 hours. The photoproducts were then extracted with acetonitrile and analyzed. The analysis indicated the ratio of photoproducts to be 1 : 1, confirming that no selective inclusion or extraction of photoproducts took place.

Discussion

We have used two methodologies, namely 'chiral inductor' and 'chiral auxiliary', to conduct enantio- and diastereoselective photocyclization of 3-dimethyl-4-oxo-3,4-dihydro-naphthalene-1-carboxylic acid derivatives (**1a**, **1b**, **2a–2e**, **2g**, **2i**, **2j**, **2m–2q**, **2s**, **2t**), 2,4-cyclohexadienone derivatives (**1c–1e**, **4a**, **4e–4h**, **4j**, **4n**, **4o**, **4q**, **4r**, **4s**) and *N*-alkyl pyridone derivatives (**1e–1j**, **6e**, **6g**, **6i–6q**) (Schemes 1–4). All three systems gave similar enantio- and diastereoselectivities by chiral inductor and chiral auxiliary approaches, and the extent of selectivity was dependent on the nature and number of cations within a zeolite, presence of water and the structure of chiral inductor/chiral auxiliary. These observations suggest that the model used to understand the asymmetric induction within zeolites should take into consideration the existence of interaction between the reaction site, the chiral component and the cation present within a zeolite.

Although the products in the three systems are different, the primary step that determines the chirality involves similar motions (Scheme 5). Naphthalenones and cyclohexadienones in their excited triplet state undergo 1,3-bonding through disrotatory motion of the p-orbitals inward or outward to yield the triplet diradical intermediate that rearranges to the final product. Pyridones yield the β-lactams from their excited singlet state *via* 1,4-bonding through disrotatory motion of the p-orbitals inward or outward by a concerted 4e-cyclization process. Once the molecule is adsorbed on the zeolite surface, the outward motion that would push the newly forming cyclopropane ring (naphthalenones and cyclohexadienones) or β-lactam ring towards the surface would not be sterically favored, and therefore once the molecule is adsorbed on a surface the cyclization is expected to proceed only

Table 5 Effect of co-adsorbent (water) on diastereoselectivity in the photoproducts[a,b]

Zeolite	Substrate	% Diastereoselectivity (dry)	% Diastereoselectivity (wet)
NaY	**2b**	48A	16A
NaY	**2c**	57B	11B
NaY	**2d**	48B	25B
NaY	**2e**	45B	21B
NaY	**2i**	35B	20B
KY	**2i**	58B	9B
NaY	**2g**	48B	15B
KY	**6l**	76A	1A

[a] A refers to first peak eluting from GC/HPLC column. [b] The loading, irradiation and extraction procedures are provided in the experimental section.

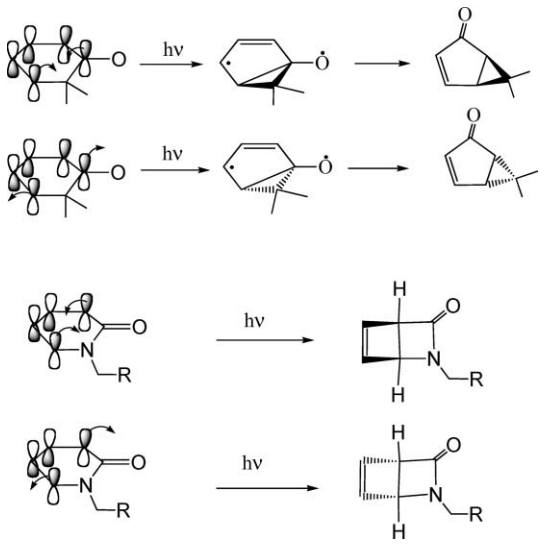

Scheme 5 Photocyclization of cyclohexadienone and pyridone.

by disrotation of the p-orbitals inward (Scheme 6). However, even this one-way rotation of the p-orbitals would yield equal amounts of the optical isomers as the reactant molecules would show no preference for adsorption from the two pro-chiral faces (Scheme 6 without chiral inductor). Interaction between the chiral inductor/chiral auxiliary and the reactant part (naphthalenone, cyclohexadienone and pyridone) could bias the adsorption process and this we believe is the origin of asymmetric induction within zeolites. We show below with the help of computational results that interaction between the chiral and reactant components mediated by cation most likely controls the asymmetric induction process. We recognize the fact that our analysis is an 'after the fact' event and the cartoon model that we envision to understand the results lacks predictive power.

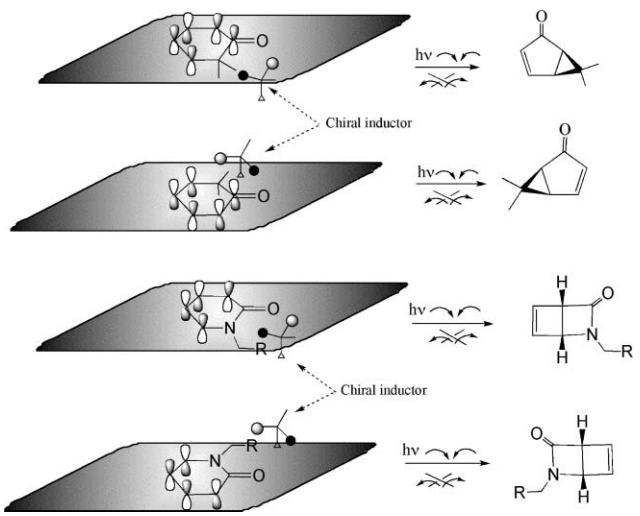

Scheme 6 Adsorption of cyclohexadienone and *N*-alkyl or aryl pyridone on a surface.

Since all three systems behaved in a similar manner, to avoid repetitive discussion, we analyze the results obtained from photocyclization of *N*-alkyl pyridone derivatives within zeolites. Irradiation of substrate **1i** within (−)-ephedrine-modified KY zeolite gave 53% excess of B enantiomer. On using the optical antipode of chiral inductor (+)-ephedrine, 50% excess of A enantiomer was obtained suggesting that the system is well behaved. Though appreciable enantioselectivity was obtained with pyridone derivatives (**1h**, **1i** and **1j**), their alkyl counter parts, namely *N*-methyl pyridone (**1e**), *N*-ethyl pyridone (**1f**) and *N*-propyl pyridone (**1g**), yielded very low enantioselectivity (3–6%) (Table 1). Furthermore, in the aryl-substituted **1h**, **1i** and **1j** the one with ethyl and propyl chain gave higher enantioselectivity than the one with single methylene unit (Table 1, ee in **1j** ~ **1i** > **1h**).

To probe the role of the phenyl group and the chain length in controlling the extent of stereoselectivity, we performed computations on substrates **1f**, **1h**, **1i** and **1j** at RB3LYP level using 6–31G* basis set with Gaussian 98 A.11 suite of programs.[20] Geometry optimized structures of the substrates were allowed to interact with Li^+ cation and the cation-bound complexes were reoptimized. During the optimization, the metal ion was free to move to find the most stable position. The optimized computed structures of Li^+ complexes with **1f**, **1h**, **1i** and **1j** are provided in Fig. 1. The computed structures indicate that the primary interaction of cation (Li^+) with the alkyl-substituted *N*-ethyl pyridone (**1f**) is with the carbonyl group *via* cation-dipolar interaction (binding affinity = 66.31 kcal mol^{-1}). However, in the cases of aryl-substituted pyridones (**1h–1j**), the cation (Li^+) interacted simultaneously with both the phenyl group (cation–π interaction) and the carbonyl group (cation-dipolar type interaction) (binding affinity = 76.66 kcal mol^{-1} for **1h**, 85.83 kcal mol^{-1} for **1i** and 85.11 kcal mol^{-1} for **1j**). In terms of the origin of the difference in the extent of enantioselectivity between the two systems, a comparison of the structures of **1f**–Li^+ and **1h**–Li^+ is revealing. The best ee for **1f** is 6%, while for **1h** is 22%. In **1f**, the cation interacts only with carbonyl chromophore leaving the ethyl substituent free. On the other hand, in **1h** the cation ties up the molecule by interacting with the carbonyl and the phenyl group. Clearly when cation rigidifies the reactant molecule as a whole, the chiral inductor is able to force it to prefer one mode of adsorption at the expense of the other (Fig. 1, Scheme 6). As indicated by the results of **1i** and **1j**, stronger

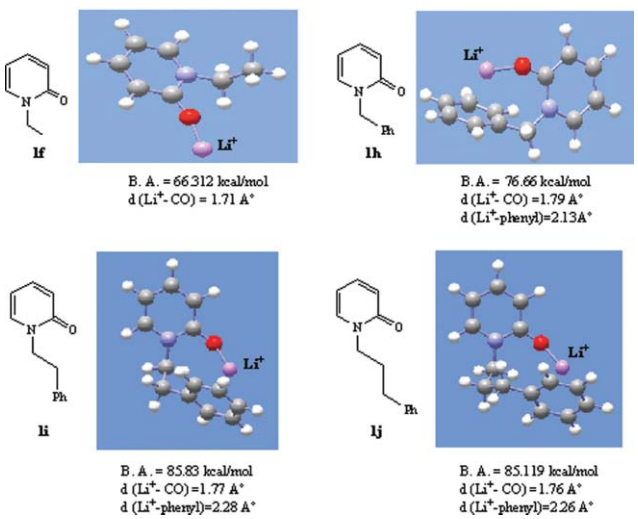

Fig. 1 Interaction of Li^+ with *N*-ethyl pyridone (**1f**), *N*-benzyl pyridone (**1h**), *N*-ethyl phenyl pyridone (**1i**) and *N*-propyl phenyl pyridone (**1j**). The structures have been computed at RB3LYP/631G* level using Gaussian 98. B. A. refers to binding affinity.[20]

binding leads to higher ee. In both cases, binding affinity is ~85 kcal mol^{-1}, and the highest ee in both cases is ~50% (Table 1).

We had shown previously through solid-state NMR (CP–MAS) and computational results that Li^+ bound cyclohexyl phenyl ketone binds to chiral inductors such as norephedrine in a very specific manner.[21] We believe that a similar ternary complex is formed between the reactant pyridone, Li^+ and the chiral inductor. Since Li^+ is bound both to the carbonyl and the phenyl groups, the chiral inductor would be favored to interact from the same side where the substituent is present. Approach from this side, due to steric considerations, would force the pyridone to selectively adsorb from the less hindered pro-chiral face, leading to enantiomeric excess in the product. In the case of **1f** where the Li^+ interacts only with the carbonyl chromophore, the chiral inductor most likely would bind to the carbonyl of the pyridone from the unsubstituted side, leading to no preference in the adsorption mode. This intuitive model explains the high ee in **1h**, **1i** and **1j** and the low values in **1e**, **1f** and **1g**.

Linking the chiral auxiliaries to the cyclohexadienone, naphthalenone and pyridone derivatives did not lead to appreciable chiral induction in solution (Tables 2, 3 and 4) suggesting a lack of communication between the two parts of the molecule in this media. On the other hand, irradiation of the same substrates as zeolite complexes resulted in a significant enhancement in diastereoselectivity. For example, **2g** gave 81% (KY zeolite) while **4f** and **6l**, gave 73% (NaY zeolite) and 88% (RbY zeolite) de, respectively (Tables 2, 3 and 4). These results indicated that the confinement provided by the zeolite framework along with cation–organic interaction was able to exert a greater control over the mode of cyclization.

As observed in the chiral inductor approach, the substrates appended with a chiral auxiliary containing an aryl group gave higher diastereoselectivity as compared to chiral auxiliary with an alkyl substituent. The importance of aryl-substituted chiral auxiliary in achieving greater selectivity is demonstrated by the following example. Substrates **6g**, **6k** and **6l**, that have an aryl group, when irradiated within a zeolite gave the β-lactam product in 42% (KY), 67% (KY) and 88% (RbY) de, respectively. The substrate **6i**, that has alkyl chiral auxiliary (cyclohexyl ethyl amine), gave the β-lactam product in 24% de in LiY zeolite. To obtain an insight into the differential behavior of alkyl- and aryl-substituted chiral auxiliaries, computations at RB3LYP/631G* level were performed.[20] The computation suggested that for the substrates **6g**, **6k** and **6l**, the cation (Li^+) interacted with the carbonyl group of the chiral auxiliary, carbonyl group of the pyridone and the phenyl group of the chiral auxiliary through cation–π interaction (Fig. 2) (binding affinities of **6g**, **6k** and **6l** are 89.74 kcal mol^{-1}, 92.66 kcal mol^{-1} and 96.36 kcal mol^{-1}). This type of interaction, that ties up the reactant part and the chiral information together, suppresses the conformational flexibility of the chiral auxiliary. When the phenyl group is replaced by a cyclohexyl group (example **6i**), the cation–π interaction between the cation and the phenyl group is switched off (Fig. 3) and the de decreased. The cation now interacts primarily with either the pyridone part (binding affinity = 65.36 kcal mol^{-1}) or the carbonyl group of the chiral auxiliary (binding affinity = 63.36 kcal mol^{-1}). This type of interaction does not restrict the flexibility of the chiral auxiliary. From this comparison it is clear that mobility of chiral auxiliary should be restricted for it to be effective. In

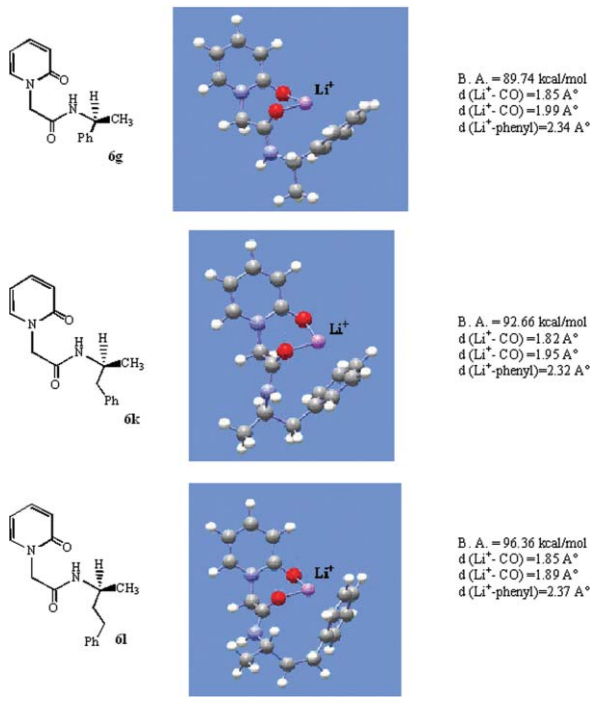

Fig. 2 Interaction of Li^+ with substrates **6g**, **6k** and **6l**. The structures have been computed at RB3LYP/631G* level using Gaussian 98. B. A. refers to binding affinity.

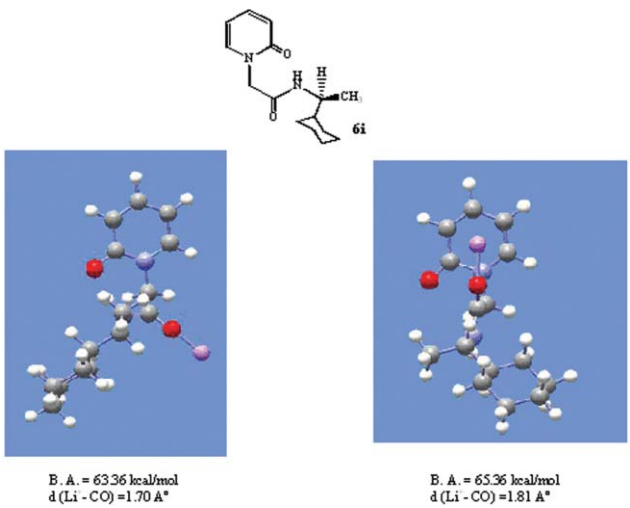

Fig. 3 Interaction of Li^+ with substrate **6i**. The structures have been computed at RB3LYP/631G* level using Gaussian 98. B. A. refers to binding affinity.

the presence of a chiral auxiliary, especially when its mobility is restricted, as in **6g**, **6k** and **6l**, and it is tied to the reactant site through cation–CO–aromatic interactions, the two prochiral faces would not be equivalent. Under such conditions, the pyridone part of the molecule is expected to adsorb on the zeolite surface preferentially through one pro-chiral face, leading to significant asymmetric induction. However, when the flexibility of the chiral auxiliary is not restricted, as in **6i**, selective adsorption is less likely and de is expected to be low.

As observed in substrates **6g**, **6k** and **6l**, the number of methylene units connecting the chiral carbon of the amine to the

phenyl group in the chiral auxiliary has an effect on the extent of diastereoselectivity. The prominent difference between these three substrates lies in the number of methylene units (two in **6l**, one in **6k** and zero in **6g**) that links the chiral carbon of the amine to the phenyl group in the chiral auxiliary. With the increase in chain length, the phenyl group would be in a better arrangement to interact with the cation that is bound to the carbonyls of the pyridone and amide units. Consistent with this, the binding affinity values for **6g**, **6k** and **6l** to Li^+ showed an increase with the number of methylene units (binding affinity of **6g**, **6k** and **6l** are 89.74 kcal mol^{-1}, 92.66 kcal mol^{-1} and 96.36 kcal mol^{-1}, Fig. 2). Stronger interaction translates into more restriction of the chiral auxiliary and better de in the photoproduct. The phenomenon observed here is similar to that observed during chiral inductor approach with substrates **1h**, **1i** and **1j**, with the only difference being the chiral source is within the molecule. Though the calculations were performed with Li^+ cations, the other charge-compensating alkali metal ions are also expected to have a similar type of interaction with the organic molecule as with the case of Li^+ cations.

As mentioned earlier, the nature of the cation not only controlled the extent of diastereoselectivity but in examples **4f**, **4g**, **4h**, **4o**, **4q**, **6l**, and **6m**, it also controlled the diastereomer being enhanced. It has been reported in the literature that Li^+ and Na^+ bind differently to amino acids such as glycine, valine and arginine compared to K^+. Li^+ binds to these molecules preferentially through CO, NH_2 (*N*-, *O*-coordination) whereas K^+ binds to the oxygens of the COOH group (*O*-, *O*-coordination).[22–24] This could be the reason for observing cation-dependent diastereomeric switch in these substrates. Results along the same lines were obtained during the photoisomerization of 2β, 3β-diphenylcyclopropane-1α-carboxylic acid derivatives[25] and γ-hydrogen abstraction reaction of α-oxoamides within zeolites.[26]

The results presented in this report on the photocyclization of dienones, naphthalenones and *N*-alkyl pyridones within zeolites compliment our earlier investigations on the photocyclization of tropolone derivatives,[27] the geometric isomerization of 1,2-diphenylcyclopropanes[25] and 2,3-diphenyl-1-benzoyl cyclopropanes,[28] and the Norrish type II reaction of α-oxoamides,[29] phenyl adamantyl ketones,[30] phenyl norbornyl ketones and phenyl cyclohexyl ketones.[31] With the help of these examples, we have established the importance of zeolite and its charge compensating cations in effecting chiral induction in photochemical reactions. In spite of this, we are still unable to formulate rules that could help us to predict the outcome of a photoreaction within a zeolite.

Experimental

Loading and photolysis procedure

All photolysis experiments were carried out by using a 450 Watt medium pressure mercury arc lamp placed in a water-cooled pyrex immersion well.

Chiral inductor approach—solution reaction

The solution reactions were performed in acetonitrile solvent. The typical irradiation procedure is as follows. For enantiomeric excess studies, 1.5 mg of the substrates along with 15 mg of the chiral inductor were taken in 4 ml of acetonitrile solvent. The samples were then irradiated using a 450 W medium pressure mercury arc lamp in a water-cooled immersion well. The chiral inductor was removed by performing a column using silica gel with hexane–ethyl acetate solvent mixture. The stereoselectivity obtained in the product was measured using HPLC/GC. The conditions used for measuring the enantiomeric excess are provided in Table S1 (see ESI†). The enantiomeric or diastereomeric excesses were determined using the formula:

[(area of A − area B)/(area of A + area of B)] × 100.

A and B refer to the first and second peak of the product enantiomers/diastereomers.

Chiral inductor approach within zeolites

Chiral inductor (10–15 mg or 20–30 mg) and substrates (**1a–1j**) (1.5–2.0 mg or 2.0–2.5 mg) were dissolved in 0.5 ml of dichloromethane followed by the addition of 15 ml of hexanes. MY (Li^+, Na^+, K^+, Rb^+ and Cs^+) zeolite (150 mg or 300 mg) activated at 500 °C for 8 h was added with stirring. The loading level of substrate was kept at one molecule for every 10 supercages. A higher ratio of the chiral inductor was employed to maximize the chances of every reactant molecule being adjacent to the chiral inductor within the supercage. After stirring the slurry for 12 h, the supernatant was analyzed for reactant and chiral inductor. Fresh hexanes were added after removing the old hexanes under nitrogen. The sample was then irradiated using a 330 nm cut-off uranyl filter for substrates **1a–1d** and a pyrex cut-off filter for substrates **1f–1j**. The irradiated slurry was filtered, and washed again with hexane. The reactant and the photoproducts were extracted from the zeolite by stirring with acetonitrile for 12 h. The extract was concentrated and the reactant and its photoproducts were separated from the chiral inductors by a microcolumn (silica gel) using hexane–ethyl acetate as eluent. The analyses were conducted by GC/HPLC fitted with chiral columns. All the samples were irradiated to achieve 30% conversion to products.

Chiral auxiliary approach—solution photolysis

2 mg of the substrate (**2** and **4**) to be irradiated was dissolved in 5 ml of trifluoroethanol, degassed with nitrogen, followed by 15–20 minutes irradiation. Conversion to photoproduct was monitored on a gas chromatograph, HP-5 capillary column. 2mg of the substrate (**6**) to be irradiated was dissolved in 5 ml of acetonitrile, degassed with nitrogen, followed by 2 h of irradiation with a pyrex cut-off filter. Conversion to photoproduct was monitored on a gas chromatograph, HP-5 capillary column.

Zeolite photolysis

The substrates (**2**, **4** and **6**) (1.5–2.0 mg or 2.0–2.5 mg) were dissolved in 0.5 ml of dichloromethane followed by addition of 15 ml of hexanes. MY (Li^+, Na^+, K^+, Rb^+ and Cs^+) zeolite (150 mg or 300 mg) activated at 500 °C for 8 h was added with stirring. The loading level of substrate was kept at one molecule for every 10 supercages. After stirring the slurry for 12 h, fresh hexanes were added to the slurry after removing the old hexanes under nitrogen. The supernatant was analyzed for the reactant. The sample was then irradiated using an appropriate filter (330 nm for substrates **2**, **4** and pyrex cut-off filter for substrates **6**) filtered,

washed again with hexanes. Substrates **2** and **4** were irradiated for 10 min. and substrates **6** were irradiated for 2 h. The reactant and the photoproducts were extracted from the zeolite by stirring with acetonitrile. The extract was concentrated and the analyses were conducted in HPLC/GC fitted with chiral columns.

Computational methods

Full geometry optimizations were carried out primarily using the hybrid Hartree–Fock density functional theory (RB3LYP) with Becke three parameter exchange functional in conjunction with correlation function by Lee, Yang and Parr. The 6–31G* basis set was used for C, H, O, N and Li. Stationary points have been characterized as true minima by frequency calculations. All the calculations were performed using Gaussian 98 A.11 suite of quantum chemical programs.[20]

Acknowledgements

V. R. thanks the NSF for financial support (CHE-0212042)

References

1 Y. Inoue, in '*Chiral Photochemistry*', ed. Y. Inoue and V. Ramamurthy, Marcel Dekker Inc., New York, 2004.
2 Y. Inoue, *Chem. Rev.*, 1992, **92**, 741.
3 H. Rau, in '*Chiral Photochemistry*', ed. Y. Inoue and V. Ramamurthy, Marcel Dekker Inc., New York, 2004.
4 B. Grosch and T. Bach, in '*Chiral Photochemistry*', ed. Y. Inoue and V. Ramamurthy, Marcel Dekker Inc., New York, 2004.
5 Y. Inoue, H. Ikeda, M. Kaneda, T. Sumimura, S. R. L. Everitt and T. Wada, *J. Am. Chem. Soc.*, 2000, **122**, 406.
6 J.-P. Pete and N. Hoffmann, in '*Chiral Photochemistry*', ed. Y. Inoue and V. Ramamurthy, Marcel Dekker Inc., New York, 2004.
7 J. R. Scheffer, in '*Chiral Photochemistry*', ed. Y. Inoue and V. Ramamurthy, Marcel Dekker Inc., New York, 2004.
8 K. Tanaka and F. Toda, in '*Organic Solid-State Reactions*', ed. F. Toda, Kluwer Academic Publishers, Dordrecht, Netherlands, 2002, pp. 1–46.
9 J. Sivaguru, A. Natarajan, L. S. Kaanumalle, J. Shailaja, S. Uppili, A. Joy and V. Ramamurthy, *Acc. Chem. Res.*, 2003, **36**, 509.
10 V. Ramamurthy, A. Natarajan, L. S. Kaanumalle, S. Karthikeyan, J. Sivaguru, J. Shailaja and A. Joy, in '*Chiral Photochemistry*', ed. V. Ramamurthy and Y. Inoue, Marcel Dekker Inc., New York, 2004.
11 H. Hart and R. K. Murray, *J. Org. Chem.*, 1970, **35**, 1535.
12 J. Griffiths and H. Hart, *J. Am. Chem. Soc.*, 1968, **90**, 3297.
13 J. Shailaja, P. H. Lakshminarasimhan, A. R. Pradhan, R. B. Sunoj, S. Jockusch, S. Karthikeyan, S. Uppili, J. Chandrasekhar, N. J. Turro and V. Ramamurthy, *J. Phys. Chem. A*, 2003, **107**, 3187.
14 E. J. Corey and J. Streith, *J. Am. Chem. Soc.*, 1964, **86**, 950.
15 R. C. De Selms and W. R. Schleigh, *Tetrahedron Lett.*, 1972, **34**, 3563.
16 R. Matsushima and K. Terada, *J. Chem. Soc., Perkin Trans. 2*, 1985, **9**, 1445.
17 F. Toda and K. Tanaka, *Tetrahedron Lett.*, 1988, **29**, 4299.
18 L.-C. Wu, C. J. Cheer, G. Olovsson, J. R. Scheffer, J. Trotter, S.-L. Wang and F.-L. Liao, *Tetrahedron Lett.*, 1997, **38**, 3135.
19 K. Tanaka, T. Fujiwara and Z. Urbanczyk-Lipkowska, *Org. Lett.*, 2002, **4**, 3255.
20 M. J. Frisch, G. W. Trucks, H. B. Schlegel, G. E. Scuseria, M. A. Robb, J. R. Cheeseman, V. G. Zakrzewski, J. A. Montgomery, Jr., R. E. Stratmann, J. C. Burant, S. Dapprich, J. M. Millam, A. D. Daniels, K. N. Kudin, M. C. Strain, O. Farkas, J. Tomasi, V. Barone, M. Cossi, R. Cammi, B. Mennucci, C. Pomelli, C. Adamo, S. Clifford, J. Ochterski, G. A. Petersson, P. Y. Ayala, Q. Cui, K. Morokuma, P. Salvador, J. J. Dannenberg, D. K. Malick, A. D. Rabuck, K. Raghavachari, J. B. Foresman, J. Cioslowski, J. V. Ortiz, A. G. Baboul, B. B. Stefanov, G. Liu, A. Liashenko, P. Piskorz, I. Komaromi, R. Gomperts, R. L. Martin, D. J. Fox, T. Keith, M. A. Al-Laham, C. Y. Peng, A. Nanayakkara, M. Challacombe, P. M. W. Gill, B. G. Johnson, W. Chen, M. W. Wong, J. L. Andres, C. Gonzalez, M. Head-Gordon, E. S. Replogle and J. A. Pople, *GAUSSIAN 98 (Revision A.11)*, Gaussian, Inc., Pittsburgh, PA, 2001.
21 (*a*) J. Shailaja, L. S. Kaanumalle, S. Karthikeyan, A. Natarajan, K. J. Ponchot, A. R. Pradhan and V. Ramamurthy, *Org. Biomol. Chem.*, 2006, **4**, 1561; (*b*) S. Hoyau and G. Ohanessian, *Chem.–Eur. J.*, 1998, **4**, 1561–1569.
22 R. A. Jockusch, A. S. Lemoff and E. R. Williams, *J. Am. Chem. Soc.*, 2001, **123**, 12255.
23 T. Wyttenbach, M. Witt and M. T. Bowers, *J. Am. Chem. Soc.*, 2000, **122**, 3458.
24 R. A. Jockusch, W. D. Price and E. R. Williams, *J. Phys. Chem. A*, 1999, **103**, 9266.
25 J. Sivaguru, R. B. Sunoj, T. Wada, Y. Origane, Y. Inoue and V. Ramamurthy, *J. Org. Chem.*, 2004, **69**, 6533.
26 A. Natarajan and V. Ramamurthy, *Org. Biomol. Chem.*, 2006, **4**, 4533.
27 A. Joy, L. S. Kaanumalle and V. Ramamurthy, *Org. Biomol. Chem.*, 2005, **3**, 3045.
28 J. Sivaguru, R. B. Sunoj, T. Wada, Y. Origane, Y. Inoue and V. Ramamurthy, *J. Org. Chem.*, 2004, **69**, 5528.
29 A. Natarajan, K. Wang, V. Ramamurthy, J. R. Scheffer and B. Patrick, *Org. Lett.*, 2002, **4**, 1443.
30 A. Natarajan, A. Joy, L. S. Kaanumalle, J. R. Scheffer and V. Ramamurthy, *J. Org. Chem.*, 2002, **67**, 8339.
31 A. Natarajan, V. Ramamurthy and J. T. Mague, *Mol. Cryst. Liq. Cryst.*, 2006, **456**, 71.

